Melting, Premelting, and Structural Transitions in Size-Selected Aluminum Clusters with around 55 Atoms

Gary A. Breaux, Colleen M. Neal, Baopeng Cao, and Martin F. Jarrold*

Department of Chemistry, Indiana University, 800 East Kirkwood Avenue, Bloomington, Indiana 47404, USA

(Received 30 November 2004; published 5 May 2005)

Heat capacities have been determined for unsupported aluminum clusters, Al_{49}^+–Al_{63}^+, from 150 to 1050 K. Peaks in the heat capacities due to melting occur between 450 and 650 K (well below the bulk melting point of 933 K). The peaks for Al_{51}^+ and Al_{52}^+ are bimodal, suggesting the presence of a premelting transition where the surface of the clusters melts around 100 K before the core. For clusters with $n > 55$ the melting temperatures suddenly drop, and there is a dip in the heat capacities due to a transition between two solid forms before the clusters melt.

DOI: 10.1103/PhysRevLett.94.173401 PACS numbers: 36.40.Ei, 61.46.+w

It is now accepted that clusters with fewer than 100 atoms can undergo a first-order melting transition from a solidlike phase to a liquidlike phase, the transition being signaled by a spike in the heat capacity due to the latent heat and a sharp increase in the mobility of the constituent atoms [1–11]. The melting transition is not singular as in the bulk, but occurs over a range, within which the liquidlike and solidlike phases coexist. In addition to melting, premelting transitions, such as surface premelting, are prevalent in simulations [12–19] where they are usually characterized by a small peak in the heat capacity at a lower temperature rather than the main melting transition. Experimental studies of cluster melting are challenging, and in the handful of studies reported so far, no examples of cluster premelting have been found. Here we report calorimetry measurements for size-selected aluminum clusters with around 55 atoms which show premelting transitions for some cluster sizes, specifically Al_{51}^+ and Al_{52}^+. In addition to these premelting transitions, we find that for clusters with more than 55 atoms there is a sharp drop in the melting temperature and a structural transition occurs before the clusters melt.

The calorimetry measurements were performed using the multicollision induced dissociation [20,21] approach recently developed in our group [10]. The aluminum cluster ions are generated by pulsed laser vaporization of a liquid aluminum target. Before exiting the source, the clusters pass through a 10 cm long temperature-variable (77–1200 K) extension where their temperature is set. After exiting the extension, the ions are focused into a quadrupole mass spectrometer where a specific cluster size is selected. The size-selected clusters are then focused into the collision cell where they are excited by numerous collisions with helium, and if their initial translational energy is high enough, they may dissociate. The undissociated parent ions and fragment ions are swept across the collision cell by a weak electric field, some exit through a small aperture and are focused into a second quadrupole mass spectrometer, where they are mass analyzed and then detected.

Mass spectra are recorded as a function of the clusters' translational energy as they enter the collision cell. The fraction of the clusters that dissociate is determined from each mass spectrum, and the translational energy required for 50% dissociation (TE50%D) is obtained from a linear regression. TE50%D is then determined as a function of the temperature of the source extension. This quantity provides a measure of the median internal energy of the clusters, and the derivative of TE50%D with respect to temperature is approximately proportional to the heat capacity. The proportionality constant is related to the fraction of the clusters' translational energy that is converted into internal energy in the collision cell, which can be estimated using an impulsive collision model [10,11,21]. The fraction is small, around 5% for the aluminum clusters studied here. Thus small changes in the clusters' internal energy are amplified and lead to large changes in the translational energy required for 50% dissociation.

Figure 1 shows plots of the heat capacities as a function of temperature for Al_{53}^+ and Al_{52}^+. The points are the experimental results (an average of 2–6 independent measurements) and the dashed lines are heat capacities calculated from statistical thermodynamics using a modified Debye model [22]. The results for Al_{53}^+ are representative of clusters which show a relatively narrow, well-defined melting transition. The peak in the heat capacity at around 620 K is attributed to melting. The total width of the transition (the temperature range over which the solid and liquid phases coexist) is around 200 K. The heat capacity of the liquid cluster (i.e., above 700 K) is larger than for the solid, primarily because of the configurational entropy of the liquid state. The solid line through the points for Al_{53}^+ is a fit with a Gaussian-based function. The peak in the heat capacity for Al_{52}^+ is broader than for Al_{53}^+ and clearly asymmetric, with a low temperature shoulder which suggests the existence of a poorly resolved peak around

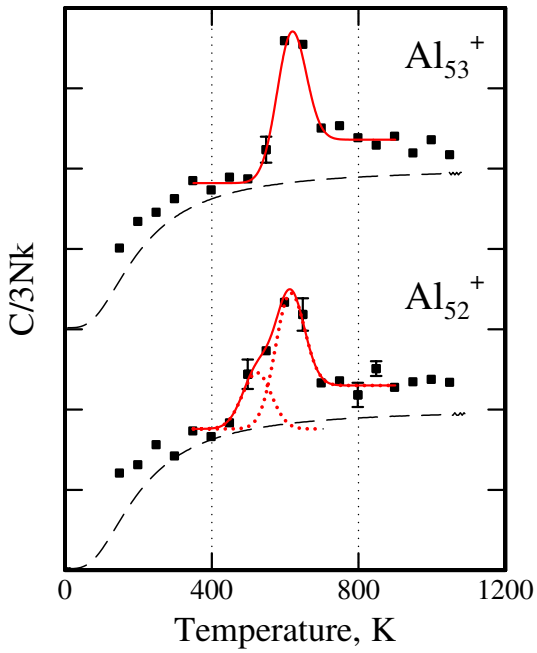

FIG. 1 (color online). Plots of heat capacities against temperature for Al_{53}^+ and Al_{52}^+. The heat capacity scale is $C/3Nk$ where $N = 3n - 6 + 3/2$, n is the number of atoms, and k is the Boltzmann's constant. The points are the experimental results and the dashed lines are calculated heat capacities derived using a modified Debye model (see text). The solid and dotted lines are fits to the results using Gaussian-based functions (see text). All the Gaussian functions have the same width.

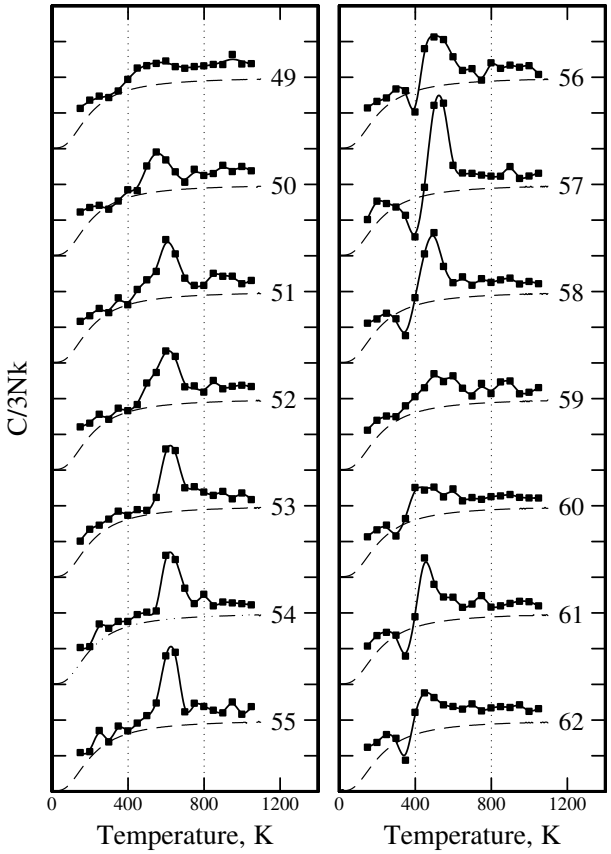

FIG. 2. Plots of the heat capacities against temperature for Al_n^+, with $n = 49$ to 62. The heat capacity scale is $C/3Nk$ where $N = 3n - 6 + 3/2$ and k is Boltzmann's constant. The points are the experimental measurements, and the dashed lines are calculated heat capacities derived using a modified Debye model (see text).

100 K lower than the main melting transition. The shoulder is evident in all six data sets recorded over the heat capacity peak for Al_{52}^+. The solid line that fits the experimental results for Al_{52}^+ was obtained by summing the two Gaussian-based functions shown by the dotted lines in Fig. 1. The small peak in the heat capacity that precedes the main melting transition is characteristic of a premelting transition.

Figure 2 shows heat capacities recorded for Al_{49}^+ to Al_{62}^+ as a function of temperature. A wide variety of different behaviors are represented, with some clusters (e.g., Al_{49}^+ and Al_{59}^+) showing poorly defined melting transitions. Clusters with 54 and 55 atoms have sharp, well-defined peaks in their heat capacities similar to that considered above for Al_{53}^+. The peak for Al_{51}^+ is similar to that for Al_{52}^+, it has a low temperature shoulder which suggests the existence of an unresolved peak around 100 K below the main melting transition. For Al_{50}^+ the peak in the heat capacity is broad but more symmetric and occurs at a significantly lower temperature than for Al_{51}^+ and Al_{52}^+. This may indicate that the peak for the main melting transition has become smaller and merged with the premelting peak. Similar behavior has been observed in some recent simulations for sodium clusters with around 130 atoms [19]. An inspection of Fig. 2 reveals that in addition to clusters with $n = 50$, 51, and 52, Al_{56}^+ also has a clearly broadened melting transition, though for this cluster (and subsequent clusters) there is also a dip in the heat capacities before the melting transition (which we discuss in more detail below).

Premelting transitions like those observed here are usually associated with surface premelting where the outermost layer of atoms melts before the core (although for small clusters, simulations suggest that geometry changes may also lead to premelting features). In the present work, premelting transitions are only observed for a small fraction of the aluminum clusters studied. We cannot explain why premelting is observed for Al_{51}^+ and Al_{52}^+, specifically, except to note that in general terms, the presence or absence of surface premelting depends on how strongly the surface atoms are bound relative to the atoms in the core [16].

Melting temperatures determined from the center of the peaks in the heat capacities are plotted in the upper half of Fig. 3. All the clusters melt at significantly below the bulk melting point of 933 K. Small particles are expected to

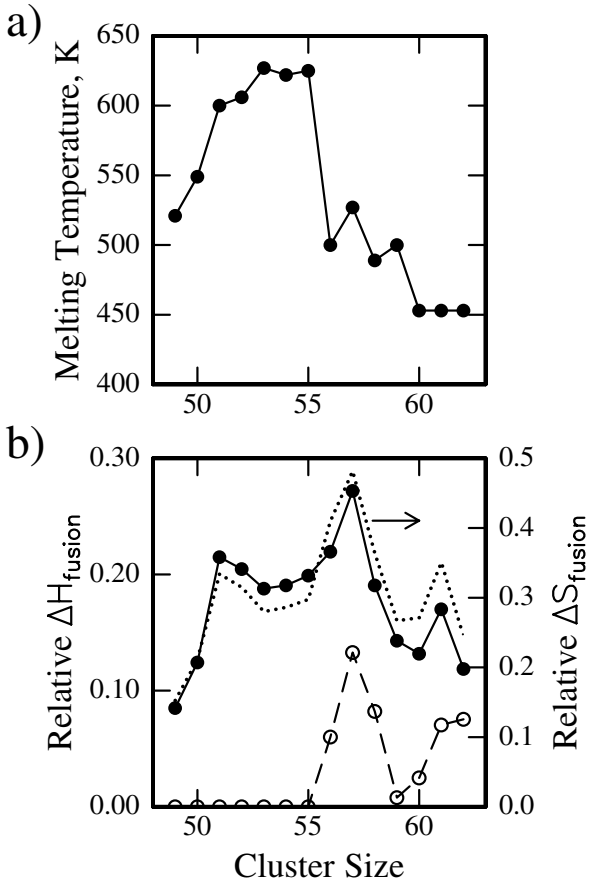

FIG. 3. (a) Plot of melting temperatures for aluminum clusters with 49–62 atoms. (b) Plot of relative heats of fusion (solid points and line) and entropies of fusion (dotted line). The open points and dashed line shows the energy change for the solid-solid transition that occurs for clusters with more than 55 atoms. These results are plotted on the same scale as the heats of fusion.

show a systematic decrease in their melting temperature with decreasing size due to the increase in their surface to volume ratio [23], though this behavior is frequently not observed in the cluster size regime. Tin and gallium clusters remain solid above the bulk melting point, which has been attributed to them having structures and bonding that are significantly different from the bulk [10,18,24,25]. Indeed, prior to this work, sodium was the only metal where experiments indicated depressed melting temperatures in the cluster size regime.

The integral of the area under the peak in the heat capacities is the heat of fusion. Heats of fusion relative to the bulk value (10.7 kJ mol^{-1} per atom) are shown plotted in lower half of Fig. 3. The heats of fusion are quite small, usually between 10% and 30% of the bulk value. Entropies of fusion, estimated from $\Delta S_{\text{fusion}} = \Delta H_{\text{fusion}}/T_{\text{melt}}$, are plotted as the dotted line in the lower half of Fig. 3. The enthalpies and entropies are closely correlated. This behavior, first reported for sodium clusters [26], appears to be a general phenomena [11]. It is evident from Fig. 2 that there is a clear maximum in the enthalpy and entropy of melting at Al_{57}^+. This cluster clearly has the most well-defined melting transition in Fig. 2. Since the enthalpy and entropy of the liquid clusters are not expected to depend strongly on the number atoms, the maxima for Al_{57}^+ are attributed to the properties of the solid cluster. In other words, solid Al_{57}^+ is a low energy and low entropy cluster.

There is sharp drop in the melting temperature between $n = 55$ and 56 (see Fig. 3). At the same point a dip appears in the heat capacities at 350–400 K, just below the melting temperature. The dip probably results from a structural change where the cluster's potential energy is significantly lowered. The lowered potential energy leads to an increase in the energy required for dissociation, which then appears as a minimum in the heat capacity. If this structural change occurred for a single cluster we would think of it as an isomerization process, however, as it emerges for a range of cluster sizes it has the character of a solid-solid phase transition where the basic structure of the lowest energy geometry changes (for example, from icosahedral to decahedral). The decrease in the potential energy associated with the solid-solid transition can be estimated by integrating over the area of the dip. The values obtained from this analysis range from 81 kJ mol^{-1} for Al_{57}^+ to 6 kJ mol^{-1} for Al_{59}^+. The energy changes for the solid-solid transition are plotted in Fig. 3(b) on the same scale as the latent heats. There is another maximum at Al_{57}^+. The stabilization of Al_{57}^+ due to the structural change is substantial. In fact, Al_{57}^+ is a particularly stable cluster, but this only emerges when the clusters are annealed almost to their melting temperature.

Since the potential energy decreases as the temperature is raised, the transition observed here is most likely an annealing transition resulting from a change in geometry from a metastable structure to the ground state structure. The metastable structure in this scenario is probably the lowest energy structure for clusters with less that 56 atoms. Presumably, as the clusters grow beyond 55 atoms they continue to follow the same growth pattern even though a lower energy structure has emerged at $n = 56$. It is necessary to heat the clusters almost to their melting point before this structure can be accessed. The sharp drop in the melting temperature at 55 atoms is probably a consequence of this geometry change. Note that the solid-solid transition converts the clusters into their lowest energy geometry before they melt. Hence the drop in the melting temperature is not due to the clusters having metastable geometries when they melt. There have been a number of theoretical studies of the structures of aluminum clusters in the size range examined here, using both empirical potentials [27–32] and density functional theory (DFT) [33–35]. There is, however, no consensus on the lowest energy geometries.

Since there is evidence for different structural forms for clusters with more than 55 atoms, we should consider whether isomers could be responsible for the multiple

peaks found in the heat capacity plots for Al_{51}^+ and Al_{52}^+. If two well-defined structures exist for a cluster they cannot have different melting points because they share a common liquid state. Thus if structure A has a lower melting temperature than structure B, when structure A melts the resulting liquid must freeze into the higher melting form. Hence there can only be one melting temperature, and all isomers should convert into the lowest energy form as the melting temperature is approached. It is possible that the structural transition we observe for clusters with more than 55 atoms is a reflection of this fact.

In summary, calorimetry measurements have revealed melting and premelting transitions for aluminum clusters with around 55 atoms. The premelting transitions, presumably surface melting, are only observed for a few cluster sizes, for example for Al_{51}^+ and Al_{52}^+. There is a sharp drop in the melting temperature for aluminum clusters with between 55 and 56 atoms. At the same point a solid-solid transition emerges before the clusters melt. The presence of the solid-solid transition suggests that there is a basic change in the structure of the lowest energy geometry at 56 atoms.

We gratefully acknowledge the support of the National Science Foundation.

*Corresponding author.
Electronic address: mfj@indiana.edu

[1] C. L. Briant and J. J. Burton, J. Chem. Phys. **63**, 2045 (1975).
[2] R. S. Berry, J. Jellinek, and G. Natanson, Chem. Phys. Lett. **107**, 227 (1984).
[3] P. Labastie and R. L. Whetten, Phys. Rev. Lett. **65**, 1567 (1990).
[4] D. J. Wales and R. S. Berry, J. Chem. Phys. **92**, 4473 (1990).
[5] D. J. Wales and R. S. Berry, Phys. Rev. Lett. **73**, 2875 (1994).
[6] R. E. Kunz and R. S. Berry, Phys. Rev. E **49**, 1895 (1994).
[7] M. Schmidt, R. Kusche, W. Kronmüller, B. von Issendorff, and H. Haberland, Phys. Rev. Lett. **79**, 99 (1997).
[8] M. Schmidt, R. Kusche, B. von Issendorff, and H. Haberland, Nature (London) **393**, 238 (1998).
[9] M. Schmidt and H. Haberland, C.R. Physique **3**, 327 (2002).
[10] G. A. Breaux, R. C. Benirschke, T. Sugai, B. S. Kinnear, and M. F. Jarrold, Phys. Rev. Lett. **91**, 215508 (2003).
[11] G. A. Breaux, D. A. Hillman, C. M. Neal, R. C. Benirschke, and M. F. Jarrold, J. Am. Chem. Soc. **126**, 8628 (2004).
[12] V. V. Nauchitel and A. J. Pertsin, Mol. Phys. **40**, 1341 (1980).
[13] H.-P. Cheng and R. S. Berry, Phys. Rev. A **45**, 7969 (1992).
[14] A. Aguado, J. M. Lopez, J. A. Alonso, and M. J. Stott, J. Chem. Phys. **111**, 6026 (1999).
[15] F. Calvo and F. Spiegelmann, J. Chem. Phys. **112**, 2888 (2000).
[16] Y. J. Lee, E.-K. Lee, and S. Kim, Phys. Rev. Lett. **86**, 999 (2001).
[17] A. Aguado, L. M. Molina, J. M. Loez, and J. A. Alonso, Eur. Phys. J. D **15**, 221 (2001).
[18] K. Joshi, D. G. Kanhere, and S. A. Blundell, Phys. Rev. B **67**, 235413 (2003).
[19] F. Calvo and F. Spiegelmann, J. Chem. Phys. **120**, 9684 (2004).
[20] M. F. Jarrold and E. C. Honea, J. Phys. Chem. **95**, 9181 (1991).
[21] M. F. Jarrold and E. C. Honea, J. Am. Chem. Soc. **114**, 459 (1992).
[22] J. Bohr, Int. J. Quantum Chem. **84**, 249 (2001).
[23] P. Pawlow, Zur Didaktik der Physik und Chemie: Vortrage auf der Tagung fur Didaktik der Physik/Chemie **65**, 545 (1909).
[24] A. A. Shvartsburg and M. F. Jarrold, Phys. Rev. Lett. **85**, 2530 (2000).
[25] S. Chacko, K. Joshi, D. G. Kanhere, and S. A. Blundell, Phys. Rev. Lett. **92**, 135506 (2004).
[26] M. Schmidt, J. Donges, Th. Hippler, and H. Haberland, Phys. Rev. Lett. **90**, 103401 (2003).
[27] J. Jellinek and A. Goldberg, J. Chem. Phys. **113**, 2570 (2000).
[28] S. K. Lai, W. D. Lin, K. L. Wu, W. H. Li, and K. C. Lee, J. Chem. Phys. **121**, 1487 (2004).
[29] J. Jellinek and A. Goldberg, J. Chem. Phys. **113**, 2570 (2000).
[30] J.-O. Joswig and M. Springborg, Phys. Rev. B **68**, 085408 (2003).
[31] J. P. K. Doye, J. Chem. Phys. **119**, 1136 (2003).
[32] K. Manninen, J. Akola, and M. Manninen, Phys. Rev. B **68**, 235412 (2003).
[33] H.-P. Cheng, R. S. Berry, and R. L. Whetten, Phys. Rev. B **43**, 10 647 (1991).
[34] J.-Y. Yi, D. J. Oh, and J. Bernholc, Phys. Rev. Lett. **67**, 1594 (1991).
[35] J. Akola, M. Manninen, H. Häkkinen, U. Landman, X. Li, and L.-S. Wang, Phys. Rev. B **62**, 13 216 (2000).